Pseudo-Heterodyne Signal Processing Scheme for Interrogation of Fibre Bragg Grating Sensor Arrays.

C.K.Chatterjea, S.W.James and R.P.Tatam
Optical Sensors Group, Centre for Photonics and Optical Engineering, School of Mechanical Engineering, Cranfield University, Cranfield, Bedford, MK43 0AL, United Kingdom

ABSTRACT

An intensity-based interrogation technique for arrays of Fibre Bragg Grating (FBG) sensors is reported. The technique is based upon each FBG forming one mirror of a Michelson interferometer. Source wavelength modulation is combined with an unbalanced interferometer to produce a carrier signal. Carrier frequencies are characteristic of the optical path length imbalance and hence grating position within the array. The intensity of the carrier signal is directly related to the optical power reflected from the grating and hence the strain applied to the grating. Strain resolution of ~3μm/m is demonstrated with a ~350μm/m sensor range. Multiplexing is demonstrated and techniques to extend the range are discussed.

Keywords: Bragg Gratings, Multiplexing, Fibre-Optic Sensors, Interferometry

1. INTRODUCTION

Fibre Bragg grating sensors are fast becoming a key technology for use in a wide variety of structural strain monitoring applications[1,2]. The majority of interrogation techniques used for this application area are based on illuminating an array of FBG's using a source with a large spectral bandwidth, typically several tens of nanometers. Wavelength-division-multiplexing (WDM) techniques are then used to measure the wavelength of light returned from each grating[3]. This technique works well for limited grating numbers; typically ~10 sensors can be unambiguously monitored if each sensor has a range of 5000μm/m. Additional sensors can be addressed by incorporating time-division-multiplexing (TDM)[4,5] and/or spatial-division-multiplexing. In both cases the individual sensor bandwidth is generally restricted to a maximum of a few hundred Hz. The limited optical power available per sensor also limits the sensor bandwidth by limiting the signal to noise ratio available. An alternative approach, that has had limited practical demonstration to date, is to interrogate the FBG's with a laser source. Now the source spectral width is much narrower then the FBG such that a change in the centre wavelength of the FBG causes a change in the intensity of the reflected light. Although intensity sensors have relatively low dynamic range (10^2 - 10^4) in comparison to interferometric and wavelength based techniques, their performance is adequate for many engineering applications. When laser interrogation is used arrays of FBG's need to be fabricated with near identical centre wavelengths and with low reflectivities to minimise crosstalk and ensure sufficient light reaches the furthest gratings in the array. TDM of identical arrays has been proposed[5] and recently demonstrated[4]. TDM is appropriate for gratings that are separated by several meters of fibre and/or have unequal physical separations. However, high speed detection and processing electronics are required which decrease the signal to noise performance.

In this paper we propose and demonstrate an alternative laser based interrogation technique based on frequency-division-multiplexing (FDM). In this method each FBG sensor forms one "mirror" in a path length imbalanced interferometer. The interferometer is illuminated with a single frequency laser source and pseudo-heterodyne signal processing implemented via modulation of the laser output wavelength. The *phase* of the carrier generated is dependent on the FBG and the environmental perturbations on both fibre arms of the interferometer. However, the *amplitude* of the carrier is primarily dependent upon the amount of light reflected from the FBG. Arrays of gratings with different optical path length imbalances can be formed, producing a range of carrier frequencies, which can be electronically demultiplexed. These FBG arrays form interferometers within interferometers or *nested* interferometers as they have recently been termed[6]. The nested interferometer arrangements described in reference 6 differ from the technique described here in that WDM is used and the FBGs are used to define the sensor region but do not themselves act as sensors.

Further author information-
R. P. Tatam (correspondance): Email: r.p.tatam@cranfield.ac.uk; WWW: http://www.cranfield.ac.uk/sme/cpoe
Telephone: +44 1234 754630; Fax: +44 1234 750728

Downloaded from SPIE Digital Library on 09 Feb 2011 to 138.250.84.47. Terms of Use: http://spiedl.org/terms

2. PRINCIPLE OF OPERATION

2.1. Background

Figure 1 shows schematically the difference in interrogation of a Bragg grating by a source with a spectral range that is broad compared to the optical bandwidth of the FBG and a source with a spectral range much smaller then the FBG bandwidth. Figure 1a shows that if the FBG centre wavelength changes, due to strain or temperature changes for example, the FBG will reflect light of a slightly different *wavelength.* There may also be a change in the reflected intensity dependent upon the source spectral profile and position of the FBG wavelength in the source spectrum. In figure 1b the reflected wavelength remains the same as the FBG wavelength moves but the reflected *intensity* changes.

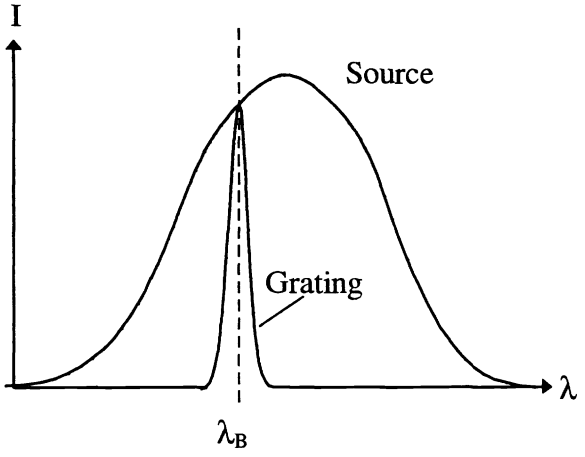

Figure 1a: Schematic illustrating a broad bandwidth source illuminating a narrow bandwidth FBG

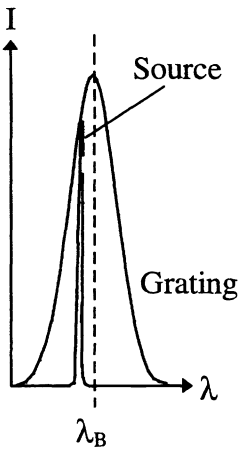

Figure 1b: Schematic illustrating a narrow bandwidth source illuminating a broad bandwidth FBG

2.2. Single Sensor Interrogation

Incorporating this effect into an interferometric interrogation technique can be understood by reference to figure 2. The optical configuration shown is a simple fibre optic Michelson interferometer formed using a directional coupler. The "mirrors" are formed by a FBG and a mirror, or a second FBG.

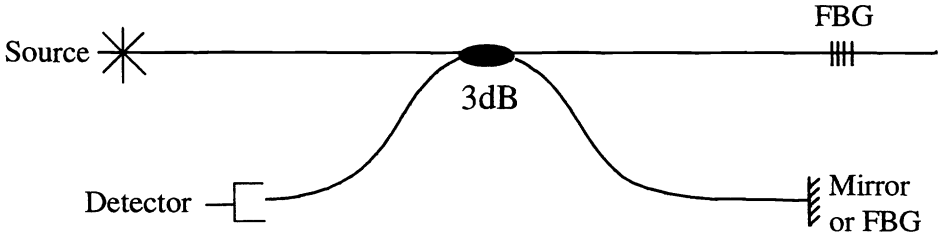

Figure 2: Optical Fibre Michelson Interferometer with a FBG mirror

This interferometer configuration behaves in a similar way to one formed using two conventional mirrors, that is, any perturbation of the fibre forming the interferometer causes a concomitant change in the interferometer phase. However, a change in the centre wavelength of the FBG causes an additional phase change and a change in the *intensity* of the returned signal. This can be seen by considering the transfer function of a two-beam interferometer:

Downloaded from SPIE Digital Library on 09 Feb 2011 to 138.250.84.47. Terms of Use: http://spiedl.org/terms

$$i_o = k(I_1 + I_2)(1 + V\cos(\varphi_m + \varphi_s)) \quad (1)$$

where I_1 and I_2 are the intensities of light at the detector from the signal path containing the FBG, and the reference path with a mirror. V is the visibility given by

$$V = \frac{2\sqrt{I_1 I_2}}{(I_1 + I_2)} \quad (2)$$

φ_s is the arbitrary interferometer phase offset, φ_m is the phase change due to modulation, i_o is the photodiode output and k is a proportionality constant dependent upon the receiver electronics.

Equations 1 and 2 show that both the fringe visibility and the intensity of the signal are dependent on I_2, i.e. the intensity of the optical power returning from the FBG sensor. The amplitude of the fringes can be calculated from the difference between the maximum and minimum interferometer output levels. Figure 3 shows the variation of this value as a function of the ratio of signal to reference intensity. As the intensity of the optical power returning from the grating increases, the photodetector output increases. The transfer function is, in general, nonlinear. However, there are regions that are approximately linear. In addition it is possible to calibrate the sensor output to correct for the non-linearity. The transfer function has a steeper gradient for low values of I_2/I_1, i.e. indicating potentially higher sensitivity for low reflectivity gratings.

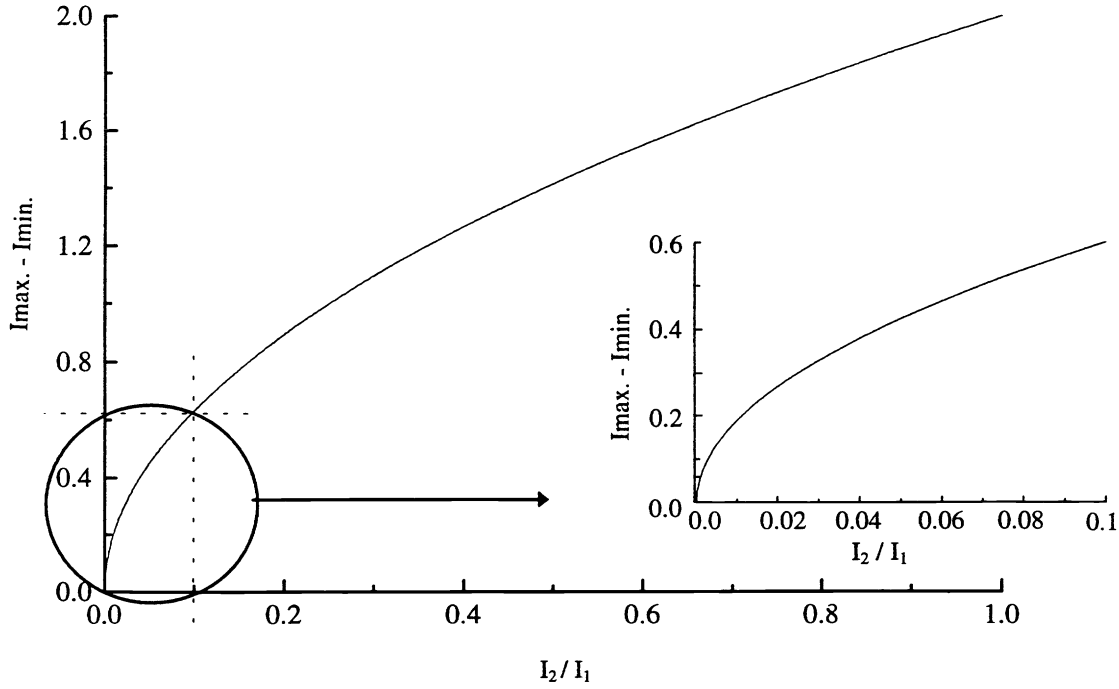

Figure 3: Fringe amplitude (Imax - Imin) plotted against the intensity ratio (I_2 / I_1)
Inset: Enlarged region I_2 / I_1 = 0 to 0.1

2.3. Signal Processing and Multiplexing

To distinguish phase changes from intensity changes requires some form of signal processing technique. Since we are interested in exploring the potential of the technique for addressing an array of sensors the signal processing method should enable multiplexing of the sensors. The method we propose here is FMCW which uses wavelength modulation of the source combined with an imbalance in the optical paths between the two interferometer arms to generate a different carrier

Downloaded from SPIE Digital Library on 09 Feb 2011 to 138.250.84.47. Terms of Use: http://spiedl.org/terms

frequency for each FBG sensor element[7,8]. The phase change, $\Delta\varphi$, in the interferometer due to an optical frequency change $\Delta\nu$, is given by

$$\Delta\varphi = \frac{2\pi\Delta L\Delta\nu}{c} \tag{3}$$

where ΔL is the optical path length imbalance and c is the free space speed of light. For a particular ΔL, $\Delta\varphi$ can be arranged to be a multiple of 2π by adjusting $\Delta\nu$ appropriately[9,10].

Modulation of the injection current of the laser with a serrodyne (sawtooth) waveform causes a linear change of the emission wavelength and a concomitant linear change in phase of the interferometer. Electrical bandpass filtering can be used to remove the higher frequencies associated with the ramp to produce a pseudo-heterodyne carrier.

All FBG's within the FDM array are written at the same central wavelength. Multiple reflections between FBG's will contribute to the carrier frequency amplitude unless careful consideration is given to the sensor array topology[11]. To reduce this crosstalk component, the optical path difference between any sensor and the reference arm mirror must be different from the physical separation of any two FBG's within the array. This is achieved as shown in figure 4 where all the FBG's are separated by equal optical path lengths. Here the optical path length in the reference arm is arranged to be equal to the optical path length to the grating B +2/3 of the length to grating C. The shortest path length imbalance in the array of interferometers is formed by the mirror and grating C. The amplitude of the injection current modulation is adjusted to produce 6π radians phase change for a path length imbalance of 3m, equivalent to 3 fringes. FBG B has an optical path length difference which produces a phase change of 4π radians, equivalent to 2 fringes. In a similar way FBG A produces 5 fringes and FBG D and E produce 4 and 7 fringes respectively. Multiple reflections between pairs of gratings give rise to frequency components at multiples of 3 fringes and can therefore be separated from the individual grating signals. The length of the reference arm of the interferometer can be chosen such that the balance point lies assymmetrically between any pair of gratings. Locating the balance position near the central array halves the maximum optical path length, hence reducing the laser phase noise component by minimising the longest optical path length imbalance.

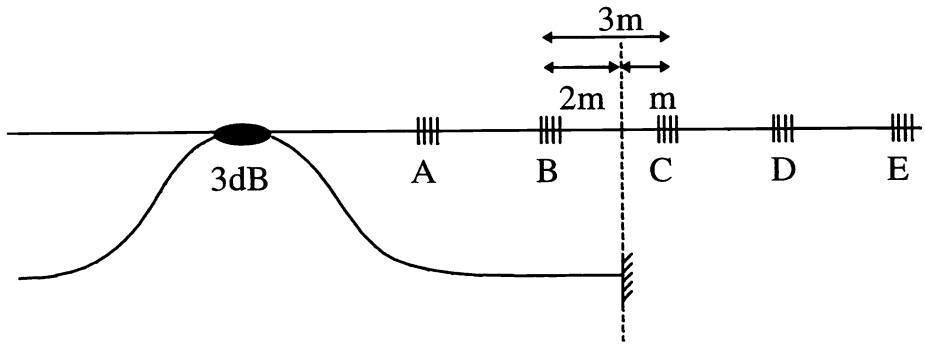

Figure 4. Schematic of nested interferometer array formed from identical gratings showing the assymetric path length imbalance used to prevent crosstalk from multiple reflections between gratings

3. EXPERIMENTAL

3.1. Single Grating Interrogation System

A schematic of the single grating interrogation system is shown in figure 5. A Sharp LT015MD 40mW, 833nm laser diode source was wavelength tuned, via temperature, down to the low wavelength side of the FBG transfer function at 830.8nm, 27mW was coupled into the single mode fibre. By utilising a tunable UV laser a FBG was fabricated to match the laser wavelength[12] , thus minimising the amount of temperature tuning required. The FBG was ~3mm long and had a bandwidth of ~0.2nm. The FBG was written into Spectran FS SMC-A0820B fibre with a reflectivity of ~10%. A directional coupler was used to form a fibre Michelson interferometer. Optical power was reflected from a mirror in one arm, and from the FBG

Downloaded from SPIE Digital Library on 09 Feb 2011 to 138.250.84.47. Terms of Use: http://spiedl.org/terms

which was mechanically spliced into the other arm to produce an optical path difference (OPD) of 0.5m. A function generator was used to apply a 3kHz serrodyne modulation frequency to the injection current. The current modulation was 1.2mA giving rise to 3GHz (0.007nm) modulation; the laser characteristics were measured to be 2.5GHz/mA using a confocal Fabry-Perot interferometer. The signal detected at the photodiode was electronically band-pass filtered and the amplitude of the carrier was measured on an oscilloscope. The fringe visibility was maximised by using a quarter wave plate in one arm of the interferometer to match the polarisation states of the signals before mixing. The FBG was mounted on a piezoelectrically controlled translation stage capable of applying ~1000μm/m across the sensor.

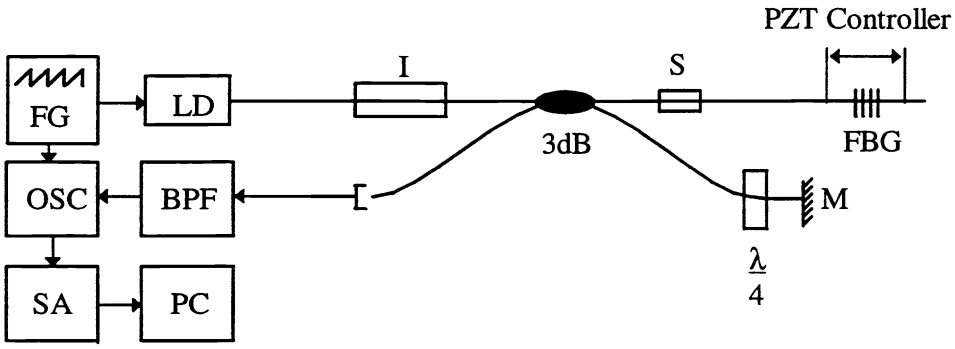

Figure 5: Experimental arrangement for single sensor configuration.
FG = Function generator, LD = Laser diode, OSC = Oscilloscope, SA = Spectrum analyser, PC = Personal computer, I = Isolator, S = Splice, M = Mirror, BPF = Band pass filter.

3.2. Multiplexing Interrogation Scheme

The source was tuned to run at high operating current and a temperature of ~24°C for optimum stability and power output. Three FBG's, spaced by 0.1m, with 20% reflectivities were side written into hydrogen loaded Spectran FS SMC-A0820B fibre[12]. The FBG array was fusion spliced to the 3dB coupler, as shown in Figure 6.

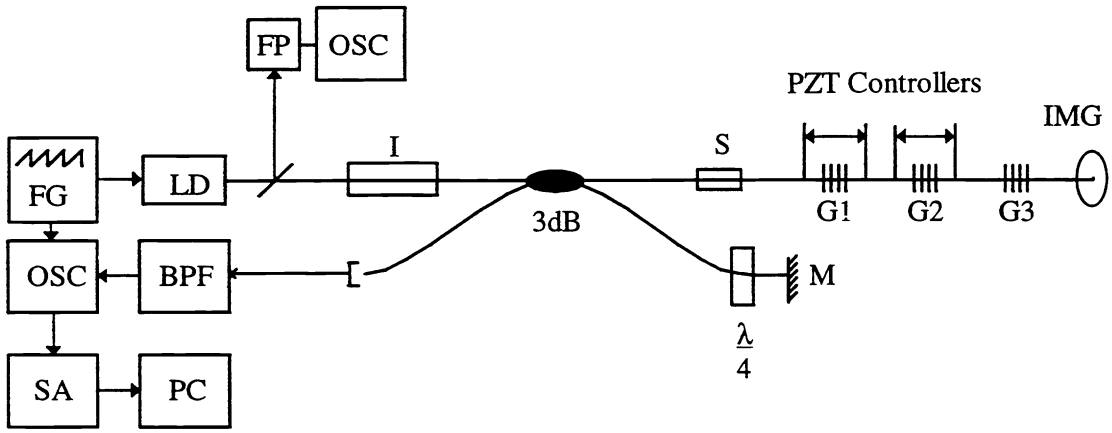

Figure 6:Experimental arrangement for multiplexed sensor array
FG = Function generator, LD = Laser diode, OSC = Oscilloscope, FP = Fabry Perot interferometer, BPF = Band pass filter SA = Spectrum analyser, PC = Personal computer, S = Splice, M = Mirror, I = Isolator, IMG = Index matching gel, Gi = FBG: ith in the array

All fibre ends were angle polished to minimise reflections back into the laser. Other fibre terminations were index matched to remove the 4% Fresnel reflection. A Faraday isolator was employed to further minimise feedback to the diode. The Sharp LT015MD laser diodes used were found to be highly sensitive to feedback, often running on multiple longitudinal modes or

Downloaded from SPIE Digital Library on 09 Feb 2011 to 138.250.84.47. Terms of Use: http://spiedl.org/terms

modes or mode hopping. The source was characterised and set, via temperature tuning, to operate in a stable regime. The laser output was monitored with a monochromator; although the monochromator output was time averaged no mode hopping was visible even over several hours of observation. A Fabry Perot etalon was incorporated into the system to monitor the laser stability during the experiment. Two of the three gratings were mounted onto PZT controlled translation stages. The fibre either side of the gratings was secured to V-grooves using Bostik superglue.

4. RESULTS

4.1. Single FBG System Results

Figures 7 and 8 show the interferometer output for the single FBG in its quiescent state and as the FBG was strained by ~400μm/m. Readings were recorded from both the oscilloscope and the spectrum analyser.

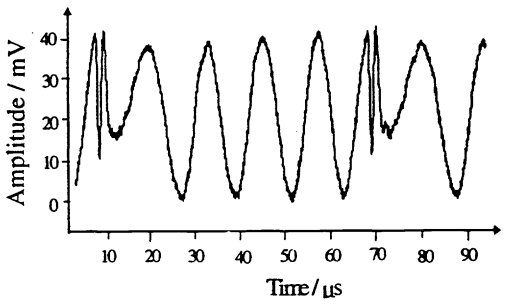

Figure 7: Oscilloscope trace showing dominant 15kHz signal

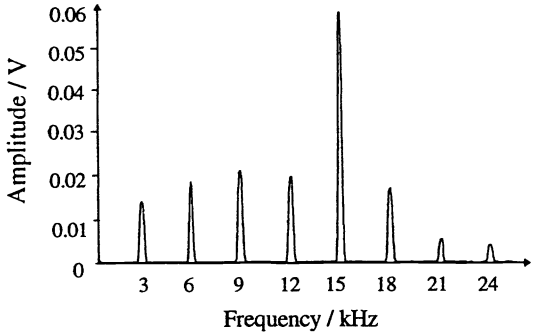

Figure 8: Frequency spectrum with dominant peak at 15kHz

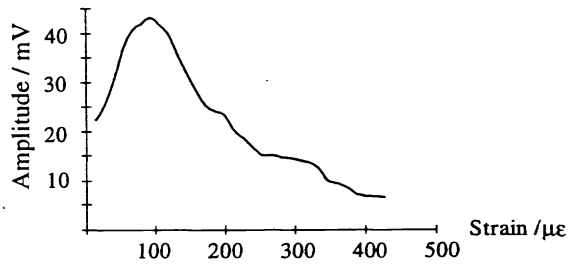

Figure 9: Carrier amplitude plotted against strain applied to the FBG measured from the oscilloscope

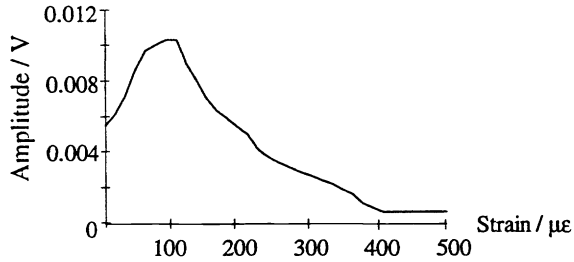

Figure 10: Carrier amplitude plotted against applied strain measured using the spectrum analyser

The measured range was 350μm/m with a resolution of ~3μm/m as recorded from the oscilloscope. Figure 7 shows the 5 fringes per ramp cycle characteristic of the OPD and modulation amplitude used. The high frequency flyback component could be filtered from the signal to reduce the noise level. An alternative way of separating the frequencies is by monitoring the system response on a spectrum analyser. Figure 8 shows the frequency spectrum with the dominant 15kHz carrier signal which, for a 3kHz ramp repetition rate, is characteristic of a 5 fringe response.

Figures 9 and 10 show the results obtained from the oscilloscope and spectrum analyser respectively, as increasing strain is applied across the grating. These results were not corrected for the non-linearity of the measurement shown in figure 3. Similar features are common for the two traces although the oscilloscope results show improved resolution due to the averaging process employed. The shape of the curve in these figures reflects the profile of the FBG.

Downloaded from SPIE Digital Library on 09 Feb 2011 to 138.250.84.47. Terms of Use: http://spiedl.org/terms

4.2. Multiplexed System Results

Traces recorded from the digital oscilloscope are shown in figure 12. The upper trace is the serrodyne waveform of the injection current applied to the diode. Figure 12b shows the 9kHz signal characteristic of multiple reflection noise in the sensor arm; this reading was taken with no light returned from the reference arm. The high frequency flyback component is evident in this waveform but, when filtered out, would produce a pure 9kHz carrier signal. Straining gratings 1 & 2 away from the interrogation wavelength enables isolation of the response of FBG G3, which is shown in figure 12c. The optical imbalance to the third FBG, G3, was set to give a 24kHz signal. It is clear from the trace shown that 8 fringes were produced by the system, thus proving the imbalance was correct. A slight modulation of the fringe amplitude is evident below the 24kHz signal. This is primarily due to remaining contributions from the other two FBG. Superposition of the noise and grating signals is demonstrated in figure 12d which shows a typical response from the system before frequency separation.

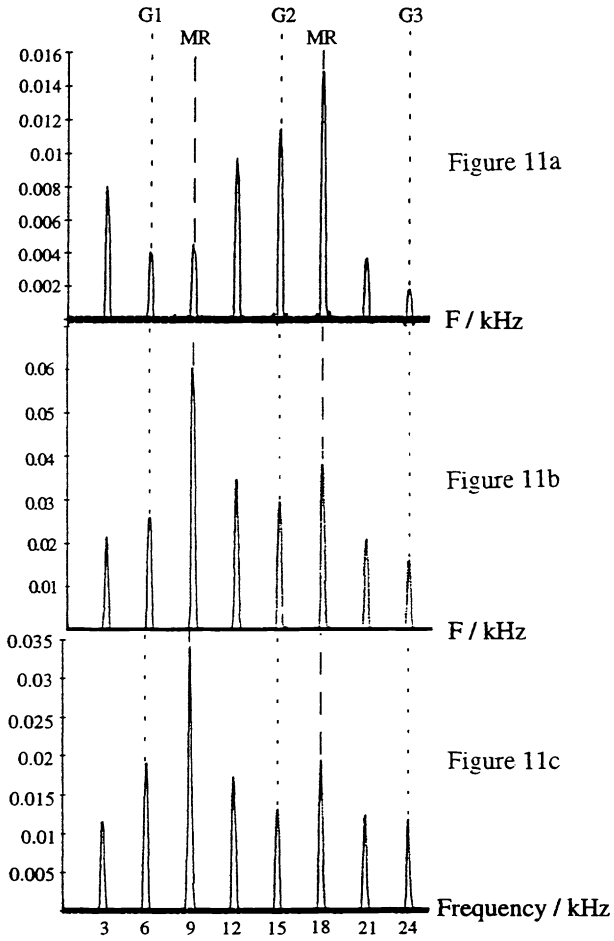

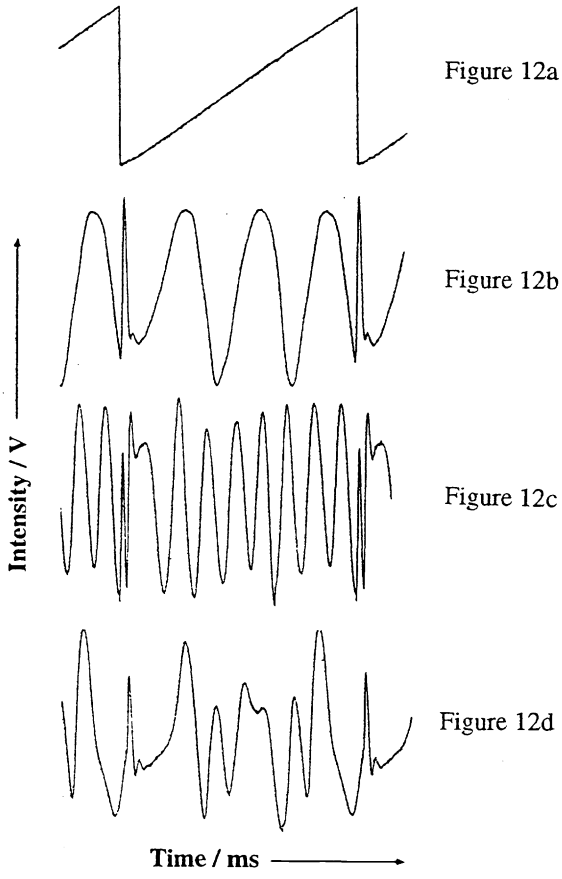

Figure 11: Spectrum analyser traces;
- 11a) Intensity increase due to grating 2 strain
- 11b) Averaged trace from system with strain grating 2
- 11c) Averaged trace from system - unstrained

MR = Multiple Reflections
Gi = FBG: ith in array

Figure 12: Oscilloscope traces;
- 12a) Injection current modulation waveform
- 12b) 9kHz (n = 3) sensor arm response
- 12c) 24kHz (n = 8) system response (G3)
- 12d) Typical system output - all frequencies

Downloaded from SPIE Digital Library on 09 Feb 2011 to 138.250.84.47. Terms of Use: http://spiedl.org/terms

The photodiode signal was also input to an electronic spectrum analyser. Figure 11c shows the system response when no strain is applied. Although the FBG reflectivities are equal, figure 11c shows a slight decrease in reflected intensity with position in the array. This is due to the intensity of the reflected optical power from each successive FBG being reduced by the transmission losses of the preceding FBG's within the array. Figure 11b shows the frequency spectrum of the system with strain applied to FBG G2. Relative changes in intensity can be seen as well as a marked increase in all the intensity values. The general rise at all frequencies is due to the increased reflection from the FBG array. Additionally the sensor arm noise signal is increased as more multiple reflections are produced. Figure 11a shows the difference in optical intensity resultant from the applied strain. The 15kHz signal, characteristic of FBG G2 optical path difference demonstrates the largest intensity increase. This is due to the reflectivity increase in response to applied strain. Increased response from FBG G1 at 6kHz is due to increased power levels in the system and the associated intensity increase in ramp harmonic signals. The FBG G3 response at 24kHz is increased the least as lower optical power levels are now transmitted through to it or received back from it. If equal optical intensities were incident on gratings 1 and 3, their responses would be identical.

5. DISCUSSION

The 350μm/m sensing range was limited by the grating bandwidth of ~0.2nm. The range could be improved by using a grating with a broad spectrum or a linear discriminator grating formed by an apodised chirped FBG[13]. These are available with linear slopes of up to 10-20nm implying a potential strain range up to 20000μm/m.

The novel topology used in this system allowed much of the multiple reflection crosstalk noise to be filtered out, reducing the crosstalk noise floor. Power budget calculations were carried out for a crosstalk noise limited system, with no additional noise sources taken into account. A serial array of up to 25 FBG's written with reflectivities of 1% would be possible. Above this the crosstalk signal would become as large as the reflected signal from the last FBG in the array. By reducing the reflectivity to 0.1%, this would rise to a 500 sensor maximum. Comparison was made of two 10 sensor arrays, one containing FBG's written at identical reflectivities, the other composed of FBG's written with decreasing reflectivity values[14]. Taking the crosstalk noise values (C/N) for the tenth sensor in the array i.e.sensor of highest loss: the decreasing reflectivities system would give C/N of 12.49dB, equivalent to 100 FBG's using the like reflectivities system. Ten identical sensors of 1% reflectivity in the latter system produced C/N of only 24.35dB which increased to 44.43dB for 0.1% reflectivities. FBG's with equal reflectivity, therefore, proved to be the superior system, as well as being far less complex to manufacture.

The nonlinear response of system intensity to strain application, shown in figure 3, was not accounted for in the results as the region of the curve which the data was recorded over closely approximated a linear response. Increased resolution is possible by calculating the sensor response for the non-linear transfer function. It has been shown that lower reflectivity FBG's increase the sensitivity of the system. The inset to figure 3 exhibits a similar transfer function with increased gradient for lower reflectivity values. Combined with the results from the crosstalk analysis, this response shows that low reflectivity FBG's can reduce crosstalk and increase system strain resolution.

Diode modulation frequencies up to several tens of GHz are possible which would enable sensing of AC measurands up into ultrasonic regimes. Further work is now being carried out to combine the FDM with WDM techniques in order to increase the number of sensors which could be interrogated for the same crosstalk limits. Unlike alternative systems involving TDM techniques, sensor separations can remain relatively short, reducing lead length and its associated noise components. In addition, no high speed electronics are required in the FDM system, a limiting factor in most TDM arrangements.

The use of birefreingent optical fibre will be required in multiplexed arrays to ensure consistent matching of the polarisation states.

The technique has the potential to be extended to measure the phase of each nested interferometer, that is, to provide measurand information integrated along the optical fibre between gratings in a similar manner to that reported in reference 6. The difference with this technique is that all the gratings have the same centre wavelength. Extending the techniques reported in this paper to provide distributed and localised information is currently under investigation.

Downloaded from SPIE Digital Library on 09 Feb 2011 to 138.250.84.47. Terms of Use: http://spiedl.org/terms

6. CONCLUSION

A novel laser based interrogation technique for arrays of identical gratings has been described. The technique used FDM to identify the gratings and measurement of the carrier amplitude to recover the wavelength shift of the grating.

C.K.Chatterjea, S.W.James and R.P.Tatam (*Optical Sensors Group, Centre for Photonics and Optical Engineering, School of Mechanical Engineering, Cranfield University, Cranfield, Bedford, MK43 0AL, United Kingdom)*

7. REFERENCES

1 P.Ferdinand, S.Magne, V.Dewynter-Marty, C.Martinez, S.Rougeault and M.Bugaud, 'Applications of Bragg Grating Sensors in Europe', *Proc:12th Int.Conf.OFS.*, **OTuB1**, pp.14-19, Williamsburg, VA., 1997.

2 M.A.Davis, T.A.Berkoff, R.T.Jones, R.L.Idriss and M.Kodinuma, 'Dynamic Strain Monitoring of an In-Use Interstate Bridge Using Fibre Bragg Grating Sensors', *Proc: SPIE* **3043**, pp.87-95, 1997.

3 A.D.Kersey, 'Interrogation and Multiplexing Techniques for Fibre Bragg Grating Strain-Sensors', *Proc: SPIE V2071,* pp.30-48, 1993.

4 A.Wilson, S.W.James and R.P.Tatam, 'Time-Division-Multiplexing of In-Fibre Bragg Gratings Using a Pulsed Laser Diode Source', *Proc: 12th Int.Conf.OFS.,* pp.475-478, Williamsburg, VA, 1997.

5 W.W.Morey, 'Distributed fibre Grating Sensors', *Proc: 7th Int.Conf. OFS.,* **Th-4**, pp.285, Sydney, Australia, 1990.

6 A.D.Kersey and M.J.Marrone, 'Bragg Grating Based Nested Fibre Interferometers', *Elec.Letts.,* **32**, pp.1221-1223, 1996.

7 I.P.Giles, D.Uttam, B.Culshaw and D.E.N.Davies, 'Coherent Optical-Fibre Sensors with Modulated Laser Sources', *Elec.Letts.*, **19**, pp.14-15, 1993.

8 D.A.Jackson, A.D.Kersey, M.Corke and J.D.C.Jones, ' Pseudo-Heterodyne Detection Scheme for Optical Interferometers', *Elec.Letts.,* **18**, pp.1081-1083, 1982.

9 A.Dandridge and L.Goldberg, 'Current-Induced Frequency Modulation in Diode Lasers', *Elec.Letts.*,**18**, pp.302-304,1982.

10 I.Sakai, 'Frequency-Division Multiplexing of Optical-Fibre Sensors Using a Frequency-Modulated Source', *Opt.&Quantum Elec.,* **18**, pp. 279-289, 1986.

11 G.Economou, R.C.Youngquist and D.E.N.Davies, 'Limitations and Noise in Interferometric Systems Using Frequency Ramped Single-Mode diode Lasers', *J.Light.Technol.*, **LT-4**, pp.1601-1608, 1986.

12 M.L.Dockney, S.W.James, R.P.Tatam, 'Fibre Bragg Gratings Facricated Using a Wavelength Tunable Laser Source and a Phase Mask Based Interferometer', *Meas.Sci.Technol.*,**7**, pp. 445-448, 1996.

13 A.D.Kersey, M.A.Davis and T.Tsai, 'Fibre Optic Bragg Grating Strain Sensor with Direct Reflectometric Interrogation', *Proc: 11th Int.Conf. O.F.S.*, Tokyo, Japan, pp.634-637, 1996.

14 R.Passy, N.Gisin, J.P.von der Weid and H.H.Gilgen, 'Experimental and Theoretical Investigations of Coherent OFDR with Semiconductor Laser Sources', *J.Light.Technol.*, **12**, pp.1622-1630, 1994.

Downloaded from SPIE Digital Library on 09 Feb 2011 to 138.250.84.47. Terms of Use: http://spiedl.org/terms